STOKES FLOW THROUGH A TWO-DIMENSIONAL CHANNEL WITH A LINEAR EXPANSION

by Elena Luca

(*Department of Mechanical and Aerospace Engineering, Jacobs School of Engineering, UCSD, La Jolla, CA 92093-0411, USA*)

and

Stefan G. Llewellyn Smith

(*Department of Mechanical and Aerospace Engineering, Jacobs School of Engineering, UCSD, La Jolla, CA 92093-0411, USA;*
Scripps Institution of Oceanography, UCSD, La Jolla, CA 92039-0213, USA.)

[Received xxx. Revise xxx]

Summary

Motivated by various applications in microfluidics, we consider low-Reynolds-number flow in a two-dimensional channel with different widths in the upstream and downstream directions. The channel geometry consists of a polygonal domain with angled edges at transition points. The polygonal nature of the geometry makes it amenable to analysis via the Unified Transform Method, providing quasi-analytical solutions which can be used to compute all the physical quantities of interest. We compute the pressure drop between the ends of the expansion or constriction region as a function of the channel width ratio and the orientation of the angled edges and compare our results to extended lubrication theory.

1. Introduction

The study of Stokes flows in confined geometries bounded by no-slip boundaries is an important area of fluid dynamics. Renewed interest in the theory of such flows has emerged as new problems arise in microfluidics applications (Kirby (**1**)).

A variety of analytical tools exist for solving two-dimensional Stokes flows and specifically in channel geometries. Davis (**2**) presented the solutions to various problems involving point singularities in a channel using Fourier transforms. The Wiener-Hopf technique which relies on Fourier transforms and factorization of functions into upper and lower analytic ones can be used to analyse problems involving mixed boundary conditions. A classical problem concerns the flow in a channel divided by a semi-infinite wall. The analysis of the symmetric channel divider reduces to a scalar Wiener-Hopf problem; this problem was originally solved by Buchwald & Doran (**3**) and Foote & Buchwald (**4**). Jeong (**5**) also analysed the flow around the semi-infinite wall in a symmetric channel divider using the Wiener-Hopf technique. Abrahams, Davis & Llewellyn Smith (**6**) considered Stokes flow in an asymmetric channel divider. The boundary value problem was reduced to a matrix Wiener-Hopf problem which was solved using Padé approximants. Kim & Chung (**7**) analysed the flow in a channel with a finite plate parallel to the walls using a three-part Wiener-Hopf formulation. Other techniques to solve problems in channel geometries

are series expansions in rectangular regions. Phillips (**8**) used the method of matched eigenfunction expansions using Papkovich-Fadle functions to study the flow in a channel with a contraction. Motivated by biological applications, Setchi *et al.* (**9**) used Papkovich-Fadle eigenfunctions associated with semi-strip geometries to solve for a variety of low-Reynolds-number flows in a channel through a shunt. For more complicated geometries, boundary integral methods have been developed and can be used to analyse the resulting flows (Pozrikidis (**10**, **11**)).

For flows in channels in which the ratio of the channel width to length is very small, the solution can be approximated by lubrication theory (Howison (**12**), Ockendon & Ockendon (**13**)). Tavakol *et al.* (**14**) have recently presented an *extended lubrication theory*, i.e. an approximation to higher-order terms, to address limitations of standard lubrication theory. They analysed low-Reynolds-number flows in channel geometries where boundaries were described by continuous and either differentiable or piecewise differentiable mathematical shape functions.

Although analytical methods can be used to solve problems in channel geometries with parallel boundaries, the analysis of problems with angled boundaries remains a challenge. Methods which rely on rectangular domain decomposition, such as the eigenfunction expansion method, can no longer be used. Lubrication theory can be used provided the width changes gradually enough. Otherwise numerical methods such as boundary integral techniques or finite difference and finite element methods have been used. Our approach gives a semi-analytical method to solve the problem of flow through channels with piecewise-straight walls.

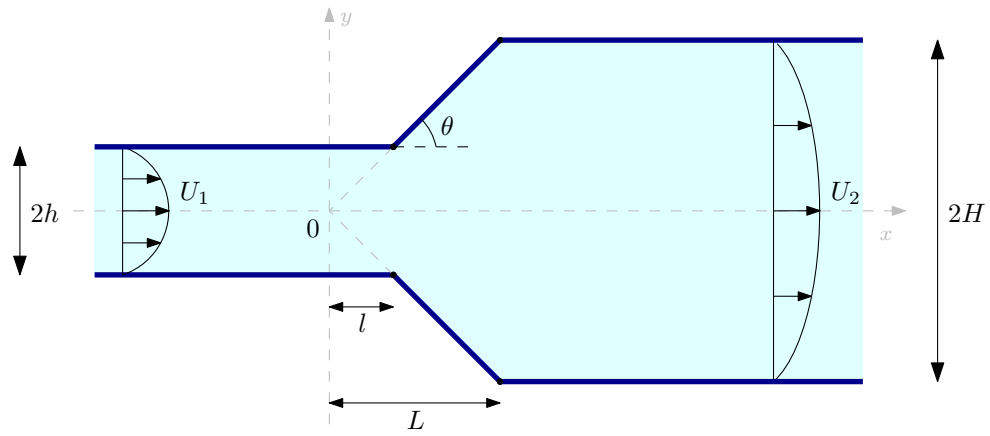

Fig. 1: Schematic of the configuration: pressure-driven flow in a polygonal channel with velocities U_1 and U_2 far upstream and downstream respectively. The transition region spans $x \in [l, L]$.

In this paper, we focus on pressure-driven Stokes flow in a two-dimensional channel with different widths in the upstream and downstream directions (Figure 1). The problem is analysed using the Unified Transform Method (UTM) which was proposed by Fokas

(**15**, **16**) and developed by Fokas and collaborators subsequently. This method provides a generalization of the classical Fourier transform, since it involves simultaneous spectral analysis with respect to two independent variables x and y. The UTM has been successfully used to solve various biharmonic boundary value problems arising in the study of Stokes flows and plane elasticity, in *convex* polygonal (**17**, **18**, **19**, **20**, **21**) and circular (**22**) domains.

Having derived the solutions using the UTM, we report computed values of the pressure drop between the ends of the expansion or constriction region as a function of the channel width ratio and the orientation of the angled edges. Our results are compared with pressure drop values found using extended lubrication theory (**14**).

2. Complex variable formulation of Stokes flow

Consider a region of incompressible fluid of viscosity μ evolving according to the Stokes equations

$$\nabla p = \mu \nabla^2 \mathbf{u}, \quad \nabla \cdot \mathbf{u} = 0, \tag{2.1}$$

where $\mathbf{u} = (u, v)$ is the two-dimensional velocity field and p is the fluid pressure. It is well-known (Langlois (**23**)) that an incompressible solution of the Stokes equations for the velocity field (u, v) can be written in terms of a stream function $\psi(x, y)$ with

$$u = \frac{\partial \psi}{\partial y}, \qquad v = -\frac{\partial \psi}{\partial x}. \tag{2.2}$$

The stream function satisfies the biharmonic equation

$$\nabla^4 \psi = 0, \tag{2.3}$$

where ∇^2 is the two-dimensional Laplacian. The general solution of (2.3) can be written

$$\psi = \mathrm{Im}[\overline{z} f(z) + g(z)], \tag{2.4}$$

where $f(z)$ and $g(z)$ are analytic functions (which can have isolated singularities) in the fluid region and are often referred to as *Goursat functions* (Langlois (**23**)). These analytic functions are related to physical quantities via

$$4f'(z) = \frac{p}{\mu} - \mathrm{i}\omega, \qquad -\overline{f(z)} + \overline{z} f'(z) + g'(z) = u - \mathrm{i}v, \tag{2.5}$$

where ω is the fluid vorticity. It is clear, then, that to solve a Stokes flow problem in two dimensions, it is sufficient to determine these two analytic functions; this is done by making use of the boundary conditions.

3. Problem formulation

Consider the two-dimensional polygonal channel shown in Figure 1 and assume that there exists a pressure-driven flow with inlet and outlet velocities, U_1 and U_2 respectively, related via the flux balance condition. The width of the channel in the upstream direction is $2h$ and in the downstream $2H$ with $H > h$. The transition region $x \in [l, L]$ consists of straight edges of direction $\pm\theta$ with respect to the real axis.

The resulting flow is symmetric about $y = 0$; this implies that the Goursat functions $f(z)$ and $g'(z)$ satisfy the following conditions

$$\overline{f}(z) = f(z), \qquad \overline{g}'(z) = g'(z), \tag{3.1}$$

where the Schwarz conjugate $\overline{h}(z)$ of a function $h(z)$ is defined by $\overline{h}(z) \equiv \overline{h(\overline{z})}$. These conditions will be used to eliminate the complex conjugate quantities that appear in the analysis of the boundary conditions.

The upper boundary of the channel of width $2H$ makes an angle $\pi - \theta$ with the expansion region (and similarly the lower boundary). If $\pi - \theta \lessapprox 146°$, one expects the emergence of recirculating regions in the vicinity of the corners, the so-called 'Moffatt eddies' (**24**). Near the corner regions, the Goursat functions have local behaviour that includes complex powers of z.

Our aim is to investigate the effect of the expansion or constriction region on the resulting flow, as well as to compute the pressure drop between its two ends.

4. Domain splitting

The first step is to split the fluid domain into three convex polygonal domains as shown in Figure 2 and write appropriate representations for the Goursat functions $f(z)$ and $g'(z)$ in each domain.

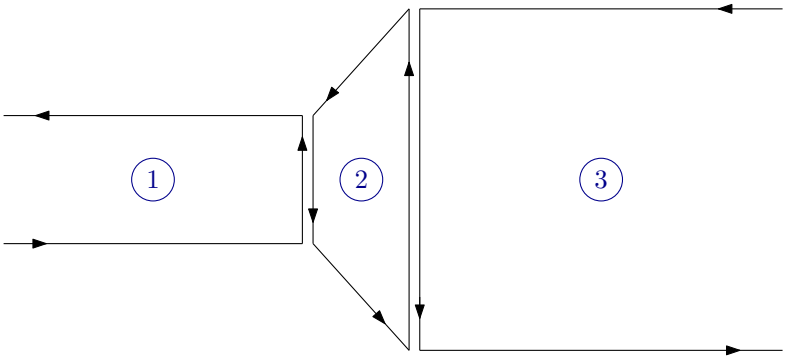

Fig. 2: Domain splitting into three sub-domains.

4.1 *Domain 1*

The Goursat functions are represented by

$$f(z) = f_u(z) + f_1(z), \qquad g'(z) = g'_u(z) + g'_1(z), \tag{4.1}$$

where $f_u(z)$, $g'_u(z)$ are known functions related to the pressure-driven flow of strength U_1 in the far field and $f_1(z)$, $g'_1(z)$ are unknown analytic functions vanishing far upstream which will be found using the transform method. The velocity components (u, v) for the pressure-driven flow of strength U_1 in the far field are given by

$$u = U_1(h^2 - y^2), \quad v = 0, \tag{4.2}$$

where U_1 is related to the flux $Q > 0$ via

$$U_1 = \frac{3Q}{4h^3} > 0. \tag{4.3}$$

The velocity field can equivalently be written in complex form as

$$u - \mathrm{i}v = \frac{U_1 z^2}{4} - \frac{U_1 z\overline{z}}{2} + \frac{U_1 \overline{z}^2}{4} + U_1 h^2, \tag{4.4}$$

with

$$f_u(z) = -\frac{U_1 z^2}{4}, \qquad g_u'(z) = \frac{U_1 z^2}{4} + U_1 h^2. \tag{4.5}$$

To find (4.5), we have compared (4.4) with the velocity expression given in (2.5). Note that there is an additive degree of freedom in the definition of the Goursat functions, since on redefining these to be

$$f(z) \mapsto f(z) + \frac{Pz}{4\mu}, \tag{4.6}$$

or

$$f(z) \mapsto f(z) + c, \qquad g'(z) \mapsto g'(z) + \overline{c}, \tag{4.7}$$

for $P \in \mathbb{R}$ and $c \in \mathbb{C}$, all the physical quantities remain unchanged. Without loss of generality, we do not add these here, but we will include them in the Goursat functions of domain 3.

Next, we use the Unified Transform Method (**16**, **25**) to represent the analytic function $f_1(z)$:

$$f_1(z) = \frac{1}{2\pi}\left[\int_0^{\infty} \rho_1(k)\mathrm{e}^{\mathrm{i}kz}\mathrm{d}k + \int_0^{-\infty} \rho_2(k)\mathrm{e}^{\mathrm{i}kz}\mathrm{d}k + \int_0^{-\mathrm{i}\infty} \rho_3(k)\mathrm{e}^{\mathrm{i}kz}\mathrm{d}k\right], \tag{4.8}$$

where the spectral functions are defined by

$$\begin{gathered}\rho_1(k) = \int_{-\infty-\mathrm{i}h}^{l-\mathrm{i}h} f_1(z)\mathrm{e}^{-\mathrm{i}kz}\mathrm{d}z, \qquad \rho_2(k) = \int_{l+\mathrm{i}h}^{-\infty+\mathrm{i}h} f_1(z)\mathrm{e}^{-\mathrm{i}kz}\mathrm{d}z, \\ \rho_3(k) = \int_{l-\mathrm{i}h}^{l+\mathrm{i}h} f_1(z)\mathrm{e}^{-\mathrm{i}kz}\mathrm{d}z.\end{gathered} \tag{4.9}$$

The spectral functions satisfy the *global relation*

$$\rho_1(k) + \rho_2(k) + \rho_3(k) = 0, \quad \mathrm{Im}[k] \geq 0. \tag{4.10}$$

Similarly, we write an integral representation for the analytic function $g_1'(z)$:

$$g_1'(z) = \frac{1}{2\pi}\left[\int_0^{\infty} \hat{\rho}_1(k)\mathrm{e}^{\mathrm{i}kz}\mathrm{d}k + \int_0^{-\infty} \hat{\rho}_2(k)\mathrm{e}^{\mathrm{i}kz}\mathrm{d}k + \int_0^{-\mathrm{i}\infty} \hat{\rho}_3(k)\mathrm{e}^{\mathrm{i}kz}\mathrm{d}k\right], \tag{4.11}$$

where the spectral functions are defined by

$$\hat{\rho}_1(k) = \int_{-\infty-\mathrm{i}h}^{l-\mathrm{i}h} g_1'(z)\mathrm{e}^{-\mathrm{i}kz}\mathrm{d}z, \qquad \hat{\rho}_2(k) = \int_{l+\mathrm{i}h}^{-\infty+\mathrm{i}h} g_1'(z)\mathrm{e}^{-\mathrm{i}kz}\mathrm{d}z,$$
$$\hat{\rho}_3(k) = \int_{l-\mathrm{i}h}^{l+\mathrm{i}h} g_1'(z)\mathrm{e}^{-\mathrm{i}kz}\mathrm{d}z. \tag{4.12}$$

The spectral functions satisfy the global relation

$$\hat{\rho}_1(k) + \hat{\rho}_2(k) + \hat{\rho}_3(k) = 0, \quad \mathrm{Im}[k] \geq 0. \tag{4.13}$$

4.2 *Domain 2*

The Goursat functions are represented by

$$f(z) = f_2(z), \qquad g'(z) = g_2'(z), \tag{4.14}$$

where $f_2(z)$, $g_2'(z)$ are analytic functions which will be found using the transform method.

Although the biharmonic equation is not conformally invariant, we use a conformal mapping to transplant the polygonal domain 2 in the z-plane to a complex parametric η-plane. The conformal mapping

$$\eta(z) = \log z \tag{4.15}$$

transplants domain 2 in the z-plane to the curvilinear domain in the η-plane shown in Figure 3. The mapping (4.15) was also used by Crowdy & Brzezicki (**21**) who analysed the Stokes flow generated by a point singularity near a semi-infinite wedge. Under this conformal mapping, the angled edges in the z-plane correspond to the horizontal edges S_1, S_3 in the η-plane and the vertical edges (in z-plane) to the curved sides S_2, S_4 (in η-plane). The parameters $a, b \in \mathbb{R}$ are defined by

$$a = \log\sqrt{l^2 + h^2}, \qquad b = \log\sqrt{L^2 + H^2}. \tag{4.16}$$

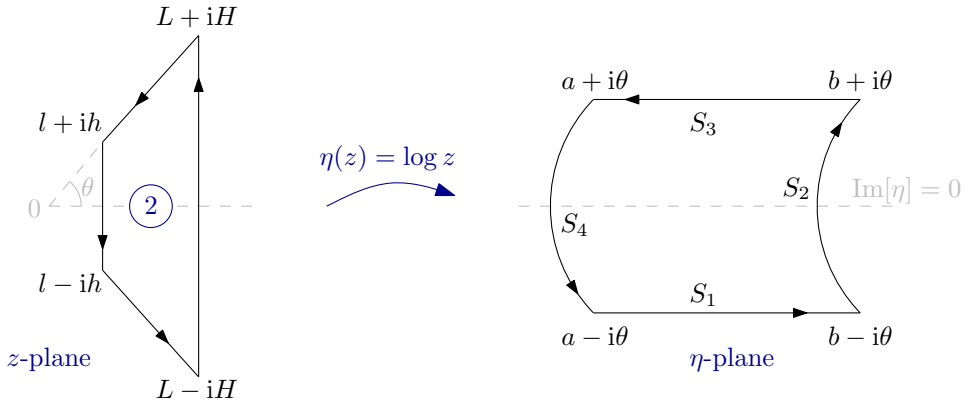

Fig. 3: Conformal mapping from the polygonal domain 2 in the z-plane to a curvilinear domain in the parametric η-plane.

Introduce the composite functions

$$F_2(\eta) \equiv f_2(z(\eta)), \qquad G_2(\eta) \equiv g_2'(z(\eta)). \tag{4.17}$$

Next, introduce the spectral functions

$$\sigma_j(k) = \int_{S_j} F_2(\eta) \mathrm{e}^{-\mathrm{i}k\eta} \mathrm{d}\eta, \quad j = 1, 2, 3, 4, \tag{4.18}$$

where S_j, $j = 1, 2, 3, 4$, denotes side j with counterclockwise orientation as shown in Figure 3. The spectral functions satisfy the global relation

$$\sum_{j=1}^{4} \sigma_j(k) = 0, \quad k \in \mathbb{C}. \tag{4.19}$$

Similarly, we write

$$\hat{\sigma}_j(k) = \int_{S_j} G_2(\eta) \mathrm{e}^{-\mathrm{i}k\eta} \mathrm{d}\eta, \quad j = 1, 2, 3, 4 \tag{4.20}$$

and the global relation

$$\sum_{j=1}^{4} \hat{\sigma}_j(k) = 0, \quad k \in \mathbb{C}. \tag{4.21}$$

Integral representations for the Goursat functions $f_2(z)$, $g_2'(z)$ will be presented in Section 6.4.

4.3 *Domain 3*

The Goursat functions are represented by

$$f(z) = f_d(z) + f_3(z), \qquad g'(z) = g_d'(z) + g_3'(z), \tag{4.22}$$

where $f_d(z)$, $g_d'(z)$ are known functions related to the pressure-driven flow of strength U_2 in the far field with some additive constants and $f_3(z)$, $g_3'(z)$ are unknown analytic functions vanishing downstream which will be found using the transform method. The functions $f_d(z)$, $g_d'(z)$ are given by

$$f_d(z) = -\frac{U_2 z^2}{4} + Pz + c, \qquad g_d'(z) = \frac{U_2 z^2}{4} + U_2 H^2 + \overline{c}, \tag{4.23}$$

where $P \in \mathbb{R}$ and $c \in \mathbb{C}$ are unknown constants which will be found as part of the solution. We note that the symmetry conditions imply that $c \in \mathbb{R}$. Using the flux balance condition, we find that U_2 is related to U_1 via

$$U_2 = \left(\frac{h}{H}\right)^3 U_1. \tag{4.24}$$

The analytic function $f_3(z)$ can be represented by

$$f_3(z) = \frac{1}{2\pi} \left[\int_0^{\infty} \tau_1(k) \mathrm{e}^{\mathrm{i}kz} \mathrm{d}k + \int_0^{-\infty} \tau_2(k) \mathrm{e}^{\mathrm{i}kz} \mathrm{d}k + \int_0^{\mathrm{i}\infty} \tau_3(k) \mathrm{e}^{\mathrm{i}kz} \mathrm{d}k \right], \tag{4.25}$$

where spectral functions are defined by

$$\tau_1(k) = \int_{L-\mathrm{i}H}^{\infty-\mathrm{i}H} f_3(z)\mathrm{e}^{-\mathrm{i}kz}\mathrm{d}z, \qquad \tau_2(k) = \int_{\infty+\mathrm{i}H}^{L+\mathrm{i}H} f_3(z)\mathrm{e}^{-\mathrm{i}kz}\mathrm{d}z, \\ \tau_3(k) = \int_{L+\mathrm{i}H}^{L-\mathrm{i}H} f_3(z)\mathrm{e}^{-\mathrm{i}kz}\mathrm{d}z. \tag{4.26}$$

The spectral functions satisfy the global relation

$$\tau_1(k) + \tau_2(k) + \tau_3(k) = 0, \quad \mathrm{Im}[k] \leq 0. \tag{4.27}$$

Similarly, we write

$$g_3'(z) = \frac{1}{2\pi}\left[\int_0^{\infty} \hat{\tau}_1(k)\mathrm{e}^{\mathrm{i}kz}\mathrm{d}k + \int_0^{-\infty} \hat{\tau}_2(k)\mathrm{e}^{\mathrm{i}kz}\mathrm{d}k + \int_0^{\mathrm{i}\infty} \hat{\tau}_3(k)\mathrm{e}^{\mathrm{i}kz}\mathrm{d}k\right], \tag{4.28}$$

where spectral functions are defined by

$$\hat{\tau}_1(k) = \int_{L-\mathrm{i}H}^{\infty-\mathrm{i}H} g_3'(z)\mathrm{e}^{-\mathrm{i}kz}\mathrm{d}z, \qquad \hat{\tau}_2(k) = \int_{\infty+\mathrm{i}H}^{L+\mathrm{i}H} g_3'(z)\mathrm{e}^{-\mathrm{i}kz}\mathrm{d}z, \\ \hat{\tau}_3(k) = \int_{L+\mathrm{i}H}^{L-\mathrm{i}H} g_3'(z)\mathrm{e}^{-\mathrm{i}kz}\mathrm{d}z. \tag{4.29}$$

The spectral functions satisfy the global relation

$$\hat{\tau}_1(k) + \hat{\tau}_2(k) + \hat{\tau}_3(k) = 0, \quad \mathrm{Im}[k] \leq 0. \tag{4.30}$$

5. Boundary conditions and spectral analysis

In this section, we will obtain more information about the spectral functions by making use of the boundary conditions. The global relations will also be used to reduce the number of unknown spectral functions.

5.1 *Domain 1*

The no-slip boundary condition on the channel boundaries can be expressed as

$$-\overline{f(z)} + \overline{z}f'(z) + g'(z) = 0, \qquad \text{on } \overline{z} = z + 2\mathrm{i}h \text{ and } \overline{z} = z - 2\mathrm{i}h. \tag{5.1}$$

On substitution of (4.1) and use of the symmetry condition (3.1), we find that, on the lower boundary $\overline{z} = z + 2\mathrm{i}h$,

$$-f_1(z + 2\mathrm{i}h) + (z + 2\mathrm{i}h)f_1'(z) + g_1'(z) = 0. \tag{5.2}$$

We multiply (5.2) by $\mathrm{e}^{-\mathrm{i}kz}$ and integrate along the lower boundary:

$$-\int_{-\infty-\mathrm{i}h}^{l-\mathrm{i}h} f_1(z + 2\mathrm{i}h)\mathrm{e}^{-\mathrm{i}kz}\mathrm{d}z + \int_{-\infty-\mathrm{i}h}^{l-\mathrm{i}h} (z + 2\mathrm{i}h)f_1'(z)\mathrm{e}^{-\mathrm{i}kz}\mathrm{d}z + \int_{-\infty-\mathrm{i}h}^{l-\mathrm{i}h} g_1'(z)\mathrm{e}^{-\mathrm{i}kz}\mathrm{d}z = 0. \tag{5.3}$$

This can be written in terms of the spectral functions as

$$\mathrm{e}^{-2kh}\rho_2(k) - \frac{\partial[k\rho_1(k)]}{\partial k} - 2kh\rho_1(k) + \hat{\rho}_1(k) + (l+\mathrm{i}h)f_1(l-\mathrm{i}h)\mathrm{e}^{-\mathrm{i}k(l-\mathrm{i}h)} = 0. \tag{5.4}$$

Similarly, on the upper boundary $\overline{z} = z - 2\mathrm{i}h$, we have

$$-f_1(z-2\mathrm{i}h) + (z-2\mathrm{i}h)f_1'(z) + g_1'(z) = 0. \tag{5.5}$$

We multiply (5.5) by $\mathrm{e}^{-\mathrm{i}kz}$ and integrate along the upper boundary:

$$-\int_{l+\mathrm{i}h}^{-\infty+\mathrm{i}h} f_1(z-2\mathrm{i}h)\mathrm{e}^{-\mathrm{i}kz}\mathrm{d}z + \int_{l+\mathrm{i}h}^{-\infty+\mathrm{i}h} (z-2\mathrm{i}h)f_1'(z)\mathrm{e}^{-\mathrm{i}kz}\mathrm{d}z + \int_{l+\mathrm{i}h}^{-\infty+\mathrm{i}h} g_1'(z)\mathrm{e}^{-\mathrm{i}kz}\mathrm{d}z = 0. \tag{5.6}$$

This can be written in terms of the spectral functions as

$$\mathrm{e}^{2kh}\rho_1(k) - \frac{\partial[k\rho_2(k)]}{\partial k} + 2kh\rho_2(k) + \hat{\rho}_2(k) - (l-\mathrm{i}h)f_1(l+\mathrm{i}h)\mathrm{e}^{-\mathrm{i}k(l+\mathrm{i}h)} = 0. \tag{5.7}$$

Addition of (5.4) and (5.7) and use of the global relations (4.10) gives (after rearrangement):

$$2[\sinh(2kh) - 2kh]\rho_1(k) = W_1(k), \qquad \mathrm{Im}[k] \geq 0, \tag{5.8}$$

where

$$\begin{aligned} W_1(k) =& [\mathrm{e}^{-2kh} + 2kh]\rho_3(k) - \frac{\partial[k\rho_3(k)]}{\partial k} + \hat{\rho}_3(k) \\ & - (l+\mathrm{i}h)f_1(l-\mathrm{i}h)\mathrm{e}^{-\mathrm{i}k(l-\mathrm{i}h)} + (l-\mathrm{i}h)f_1(l+\mathrm{i}h)\mathrm{e}^{-\mathrm{i}k(l+\mathrm{i}h)}. \end{aligned} \tag{5.9}$$

5.2 *Domain 2*

The no-slip boundary condition on the horizontal boundaries of the curvilinear domain in the η-plane (which correspond to the angled no-slip boundaries in the z-plane) can be expressed as

$$-\overline{F_2(\eta)} + \mathrm{e}^{\overline{\eta}}\frac{\partial}{\partial z}F_2(\eta) + G_2(\eta) = 0, \quad \text{on } \overline{\eta} = \eta + 2\mathrm{i}\theta \text{ and } \overline{\eta} = \eta - 2\mathrm{i}\theta. \tag{5.10}$$

Using

$$z\frac{\partial}{\partial z} = \frac{\partial}{\partial \eta} \tag{5.11}$$

and the symmetry condition (3.1) (the symmetry with respect to $y = 0$ in the z-plane corresponds to symmetry with respect to $\mathrm{Im}[\eta] = 0$ in the η-plane), we find that, on the lower boundary $\overline{\eta} = \eta + 2\mathrm{i}\theta$,

$$-F_2(\eta + 2\mathrm{i}\theta) + \mathrm{e}^{2\mathrm{i}\theta}F_2'(\eta) + G_2(\eta) = 0. \tag{5.12}$$

We multiply (5.12) by $\mathrm{e}^{-\mathrm{i}k\eta}$ and integrate along the lower boundary:

$$-\int_{a-\mathrm{i}\theta}^{b-\mathrm{i}\theta} F_2(\eta+2\mathrm{i}\theta)\mathrm{e}^{-\mathrm{i}k\eta}\mathrm{d}\eta + \mathrm{e}^{2\mathrm{i}\theta}\int_{a-\mathrm{i}\theta}^{b-\mathrm{i}\theta} F_2'(\eta)\mathrm{e}^{-\mathrm{i}k\eta}\mathrm{d}\eta + \int_{a-\mathrm{i}\theta}^{b-\mathrm{i}\theta} G_2(\eta)\mathrm{e}^{-\mathrm{i}k\eta}\mathrm{d}\eta = 0. \tag{5.13}$$

This can be written in terms of the spectral functions as

$$\mathrm{e}^{-2k\theta}\sigma_3(k)+\mathrm{i}k\mathrm{e}^{2\mathrm{i}\theta}\sigma_1(k)+\hat{\sigma}_1(k)+\mathrm{e}^{2\mathrm{i}\theta}[F_2(b-\mathrm{i}\theta)\mathrm{e}^{-\mathrm{i}k(b-\mathrm{i}\theta)}-F_2(a-\mathrm{i}\theta)\mathrm{e}^{-\mathrm{i}k(a-\mathrm{i}\theta)}]=0. \quad (5.14)$$

Similarly, on the upper boundary $\overline{\eta}=\eta-2\mathrm{i}\theta$, we have

$$-F_2(\eta-2\mathrm{i}\theta)+\mathrm{e}^{-2\mathrm{i}\theta}F_2'(\eta)+G_2(\eta)=0. \quad (5.15)$$

We multiply (5.15) by $\mathrm{e}^{-\mathrm{i}k\eta}$ and integrate along the upper boundary:

$$-\int_{b+\mathrm{i}\theta}^{a+\mathrm{i}\theta}F_2(\eta-2\mathrm{i}\theta)\mathrm{e}^{-\mathrm{i}k\eta}\mathrm{d}\eta+\mathrm{e}^{-2\mathrm{i}\theta}\int_{b+\mathrm{i}\theta}^{a+\mathrm{i}\theta}F_2'(\eta)\mathrm{e}^{-\mathrm{i}k\eta}\mathrm{d}\eta+\int_{b+\mathrm{i}\theta}^{a+\mathrm{i}\theta}G_2(\eta)\mathrm{e}^{-\mathrm{i}k\eta}\mathrm{d}\eta=0. \quad (5.16)$$

This can be written in terms of the spectral functions as

$$\mathrm{e}^{2k\theta}\sigma_1(k)+\mathrm{i}k\mathrm{e}^{-2\mathrm{i}\theta}\sigma_3(k)+\hat{\sigma}_3(k)+\mathrm{e}^{-2\mathrm{i}\theta}[F_2(a+\mathrm{i}\theta)\mathrm{e}^{-\mathrm{i}k(a+\mathrm{i}\theta)}-F_2(b+\mathrm{i}\theta)\mathrm{e}^{-\mathrm{i}k(b+\mathrm{i}\theta)}]=0. \quad (5.17)$$

Addition of (5.14) and (5.17) and use of the global relations (4.19) and (4.21) gives (after rearrangement):

$$2[\sinh(2k\theta)-k\sin(2\theta)]\sigma_1(k)=W_2(k), \qquad k\in\mathbb{C}, \quad (5.18)$$

where

$$\begin{aligned}W_2(k)=&(\mathrm{e}^{-2k\theta}+\mathrm{i}k\mathrm{e}^{-2\mathrm{i}\theta})\sigma_2(k)+(\mathrm{e}^{-2k\theta}+\mathrm{i}k\mathrm{e}^{-2\mathrm{i}\theta})\sigma_4(k)+\hat{\sigma}_2(k)+\hat{\sigma}_4(k)\\&-\mathrm{e}^{2\mathrm{i}\theta}[F_2(b-\mathrm{i}\theta)\mathrm{e}^{-\mathrm{i}k(b-\mathrm{i}\theta)}-F_2(a-\mathrm{i}\theta)\mathrm{e}^{-\mathrm{i}k(a-\mathrm{i}\theta)}]\\&-\mathrm{e}^{-2\mathrm{i}\theta}[F_2(a+\mathrm{i}\theta)\mathrm{e}^{-\mathrm{i}k(a+\mathrm{i}\theta)}-F_2(b+\mathrm{i}\theta)\mathrm{e}^{-\mathrm{i}k(b+\mathrm{i}\theta)}].\end{aligned} \quad (5.19)$$

5.3 *Domain 3*

The boundary conditions and spectral analysis are similar to those found for Domain 1. We, therefore, omit the details and report only the final key expression

$$2[\sinh(2kH)-2kH]\tau_1(k)=W_3(k), \qquad \mathrm{Im}[k]\leq 0, \quad (5.20)$$

where

$$\begin{aligned}W_3(k)=&[\mathrm{e}^{-2kH}+2kH]\tau_3(k)-\frac{\partial[k\tau_3(k)]}{\partial k}+\hat{\tau}_3(k)\\&+(L+\mathrm{i}H)f_3(L-\mathrm{i}H)\mathrm{e}^{-\mathrm{i}k(L-\mathrm{i}H)}-(L-\mathrm{i}H)f_3(L+\mathrm{i}H)\mathrm{e}^{-\mathrm{i}k(L+\mathrm{i}H)}.\end{aligned} \quad (5.21)$$

5.4 *Continuity conditions*

We impose continuity of velocity, pressure and vorticity across the common edges between domains 1 & 2 and domains 2 & 3. This is equivalent to insisting that $f(z)$ and $g'(z)$ are continuous across the common edges.

Along $z=l+\mathrm{i}y$, $y\in[-h,h]$, we have

$$f_u(z)+f_1(z)=f_2(z), \qquad g_u'(z)+g_1'(z)=g_2'(z). \quad (5.22)$$

At the corner points $z = l \pm \mathrm{i}h$, we can write

$$\begin{aligned} f_u(l - \mathrm{i}h) + f_1(l - \mathrm{i}h) &= f_2(l - \mathrm{i}h), \\ f_u(l + \mathrm{i}h) + f_1(l + \mathrm{i}h) &= f_2(l + \mathrm{i}h). \end{aligned} \tag{5.23}$$

Along $z = L + \mathrm{i}y$, $y \in [-H, H]$, we have

$$f_2(z) = f_d(z) + f_3(z), \qquad g_2'(z) = g_d'(z) + g_3'(z). \tag{5.24}$$

At the corner points $z = L \pm \mathrm{i}H$, we can write

$$\begin{aligned} f_2(L - \mathrm{i}H) &= f_d(L - \mathrm{i}H) + f_3(L - \mathrm{i}H), \\ f_2(L + \mathrm{i}H) &= f_d(L + \mathrm{i}H) + f_3(L + \mathrm{i}H). \end{aligned} \tag{5.25}$$

6. Solution scheme

In the previous section, we found the following expressions:

$$\begin{aligned} 2[\sinh(2kh) - 2kh]\rho_1(k) &= W_1(k), \qquad && \mathrm{Im}[k] \geq 0, \\ 2[\sinh(2k\theta) - k\sin(2\theta)]\sigma_1(k) &= W_2(k), \qquad && k \in \mathbb{C}, \\ 2[\sinh(2kH) - 2kH]\tau_1(k) &= W_3(k), \qquad && \mathrm{Im}[k] \leq 0. \end{aligned} \tag{6.1}$$

Using the continuity conditions (5.22)-(5.25), $W_1(k)$ and $W_3(k)$, given by (5.9) and (5.21) respectively, can be expressed in terms of spectral functions and corner values associated to domain 2.

6.1 *Conditions in the spectral k-plane*

In this section, we show how to exploit the analyticity properties of the spectral functions $\rho_1(k)$, $\sigma_1(k)$ and $\tau_1(k)$ which appear in (6.1) to identify special points in the spectral k-plane whereby information on a reduced set of unknown spectral functions is available.

The spectral function $\rho_1(k)$ is analytic in the upper half k-plane which from (6.1) means that we must require

$$W_1(k) = 0, \quad \text{for } k \in \Sigma_1 \equiv \{k \in \mathbb{C}^+ | \sinh(2kh) - 2kh = 0\}. \tag{6.2}$$

In addition, as $k \to 0$,

$$\sinh(2kh) - 2kh = \mathcal{O}(k^3), \tag{6.3}$$

which implies that $W_1(k)$ must also satisfy

$$W_1(0) = W_1'(0) = W_1''(0) = 0. \tag{6.4}$$

We note that k-points in the set Σ_1 essentially satisfy the well-known eigenvalue condition for the odd (with respect to reflection in the real axis) Papkovich-Fadle eigenfunctions of the semi-strip of width $2h$ (Spence (**26**)).

The spectral function $\sigma_1(k)$ is entire in the k-plane which means that we must require

$$W_2(k) = 0, \quad \text{for } k \in \Sigma_2 \equiv \{k \in \mathbb{C} | \sinh(2k\theta) - k\sin(2\theta) = 0\}. \tag{6.5}$$

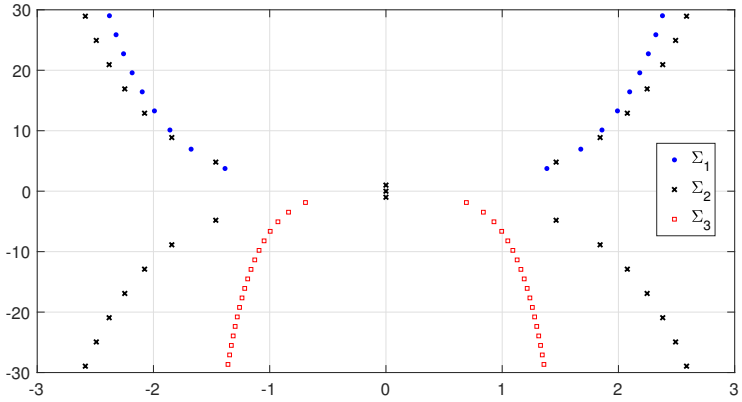

Fig. 4: Spectral k-plane and schematic of points from sets Σ_1, Σ_2 and Σ_3 given by (6.2), (6.5) and (6.8) respectively (parameters: $h = 1$, $H = 2$, $\theta = \pi/4$).

In addition, as $k \to 0$,

$$\sinh(2k\theta) - k\sin(2\theta) = \mathcal{O}(k), \tag{6.6}$$

which implies that $W_2(k)$ must also satisfy

$$W_2(0) = 0. \tag{6.7}$$

The set Σ_2 coincides with the (odd) eigenrelation found by Dean & Montagnon (**27**) and Moffatt (**24**) for the local solution near a corner of angle 2θ.

The spectral function $\tau_1(k)$ is analytic in the lower half k-plane which means that we must require

$$W_3(k) = 0, \quad \text{for } k \in \Sigma_3 \equiv \{k \in \mathbb{C}^- \,|\, \sinh(2kH) - 2kH = 0\}. \tag{6.8}$$

In addition, as $k \to 0$,

$$\sinh(2kH) - 2kH = \mathcal{O}(k^3), \tag{6.9}$$

which implies that $W_3(k)$ must also satisfy

$$W_3(0) = W_3'(0) = W_3''(0) = 0. \tag{6.10}$$

Again, the k-points of set Σ_3 satisfy the eigenvalue condition for the odd (with respect to reflection in the real axis) Papkovich-Fadle eigenfunctions of the semi-strip of width $2H$ (Spence (**26**)).

A schematic of points in the k-plane from sets Σ_1, Σ_2 and Σ_3 is given in Figure 4.

6.2 *Function representation*

We use Chebyshev expansions to represent the unknown boundary data along sides S_2 and S_4 of the mapped curvilinear domain in the η-plane.

Side S_2 can be parametrised by

$$\eta_2(s) = \log(L + \mathrm{i}Hs), \qquad s \in [-1, 1] \tag{6.11}$$

and, on this side, we write

$$\mathcal{F}_2(s) \equiv F_2(\eta_2(s)) = \sum_{m=0}^{\infty} a_m T_m(s), \qquad \mathcal{G}_2(s) \equiv G_2(\eta_2(s)) = \sum_{m=0}^{\infty} c_m T_m(s), \tag{6.12}$$

where $T_m(s) = \cos(m \cos^{-1}(s))$ is the mth Chebyshev polynomial. Similarly, side 4 can be parametrised by

$$\eta_4(s) = \log(l - \mathrm{i}hs), \qquad s \in [-1, 1] \tag{6.13}$$

and we write

$$\mathcal{F}_4(s) \equiv F_2(\eta_4(s)) = \sum_{m=0}^{\infty} b_m T_m(s), \qquad \mathcal{G}_4(s) \equiv G_2(\eta_4(s)) = \sum_{m=0}^{\infty} d_m T_m(s). \tag{6.14}$$

Using the above series expansions, it can be shown that

$$\begin{aligned} \sigma_2(k) &= \sum_{m=0}^{\infty} a_m [T(k,m)], \qquad \hat{\sigma}_2(k) = \sum_{m=0}^{\infty} c_m [T(k,m)], \\ \sigma_4(k) &= \sum_{m=0}^{\infty} b_m [U(k,m)], \qquad \hat{\sigma}_4(k) = \sum_{m=0}^{\infty} d_m [U(k,m)], \end{aligned} \tag{6.15}$$

where

$$T(k,m) = \mathrm{i}H \int_{-1}^{1} \frac{T_m(s) \mathrm{e}^{-\mathrm{i}k\eta_2(s)}}{L + \mathrm{i}Hs} \mathrm{d}s, \qquad U(k,m) = -\mathrm{i}h \int_{-1}^{1} \frac{T_m(s) \mathrm{e}^{-\mathrm{i}k\eta_4(s)}}{l - \mathrm{i}hs} \mathrm{d}s. \tag{6.16}$$

Using (6.12), (6.14) and continuity conditions (5.22), (5.24), the spectral functions $\rho_3(k), \hat{\rho}_3(k)$ and $\tau_3(k), \hat{\tau}_3(k)$ can be expressed as:

$$\begin{aligned} \rho_3(k) &= \sum_{m=0}^{\infty} b_m [P(k,m)] + \frac{U_1}{4}\, I_2(l - \mathrm{i}h, l + \mathrm{i}h, k), \\ \hat{\rho}_3(k) &= \sum_{m=0}^{\infty} d_m [P(k,m)] - \frac{U_1}{4}\, I_2(l - \mathrm{i}h, l + \mathrm{i}h, k) - U_1 h^2\, I_0(l - \mathrm{i}h, l + \mathrm{i}h, k) \end{aligned} \tag{6.17}$$

and

$$\begin{aligned} \tau_3(k) &= \sum_{m=0}^{\infty} a_m [Q(k,m)] + P\, I_1(L - \mathrm{i}H, L + \mathrm{i}H, k) - \frac{U_2}{4}\, I_2(L - \mathrm{i}H, L + \mathrm{i}H, k) \\ &\quad + c\, I_0(L - \mathrm{i}H, L + \mathrm{i}H, k), \\ \hat{\tau}_3(k) &= \sum_{m=0}^{\infty} c_m [Q(k,m)] + \frac{U_2}{4}\, I_2(L - \mathrm{i}H, L + \mathrm{i}H, k) + (U_2 H^2 + c)\, I_0(L - \mathrm{i}H, L + \mathrm{i}H, k), \end{aligned} \tag{6.18}$$

where

$$P(k,m) = \mathrm{i}h \int_{-1}^{1} T_m(s) \mathrm{e}^{-\mathrm{i}k\mathrm{e}^{\eta_4(s)}} \mathrm{d}s, \qquad Q(k,m) = -\mathrm{i}H \int_{-1}^{1} T_m(s) \mathrm{e}^{-\mathrm{i}k\mathrm{e}^{\eta_2(s)}} \mathrm{d}s \tag{6.19}$$

and the functions I_0, I_1 and I_2 are defined by

$$I_0(A,B,k) \equiv \int_A^B \mathrm{e}^{-\mathrm{i}kz} \mathrm{d}z, \qquad I_1(A,B,k) \equiv \int_A^B z\mathrm{e}^{-\mathrm{i}kz} \mathrm{d}z, \qquad I_2(A,B,k) \equiv \int_A^B z^2\mathrm{e}^{-\mathrm{i}kz} \mathrm{d}z. \tag{6.20}$$

6.3 *Formulation of a linear system*

The sums in (6.12) and (6.14) are truncated to include only terms up to $m = M$, and we formulate a linear system for the unknown coefficients $\{a_m, b_m, c_m, d_m | m = 0, ..., M\}$ and parameters P and c. The linear system comprises conditions (6.2), (6.5) and (6.8) evaluated at points in the sets $\Sigma_1, \Sigma_2, \Sigma_3$ respectively, together with conditions at $k = 0$, (6.4), (6.7) and (6.10). We found that the coefficients $\{a_m, b_m, c_m, d_m | m = 0, ..., M\}$ decay quickly and, therefore, we choose the truncation parameter to be $M = 20$.

6.4 *Computation of $f(z)$ and $g'(z)$*

Once the coefficients $\{a_m, b_m, c_m, d_m | m = 0, ..., M\}$ and parameters P and c are found, $f(z)$ and $g'(z)$ can be computed in the flow domain.

Polygonal domain 1: The spectral functions $\rho_3(k)$, $\hat{\rho}_3(k)$ can be found using (6.17). The other spectral functions, $\rho_j(k)$, $\hat{\rho}_j(k)$, $j = 1, 2$, can be computed from (5.4), (5.7) and the global relations (4.10), (4.13). Once the spectral functions are found, the correction functions $f_1(z)$, $g_1'(z)$ can be computed using (4.8) and (4.11) respectively. Finally, $f(z)$ and $g'(z)$ in domain 1 follow from (4.1).

Curvilinear domain 2: Using the analyticity properties of functions $F_2(\eta) = f_2(z(\eta))$ and $G_2(\eta) = g_2'(z(\eta))$, we extend this domain to the curvilinear domain in η-plane which is composed of a rectangle and a curvilinear domain (Figure 5).

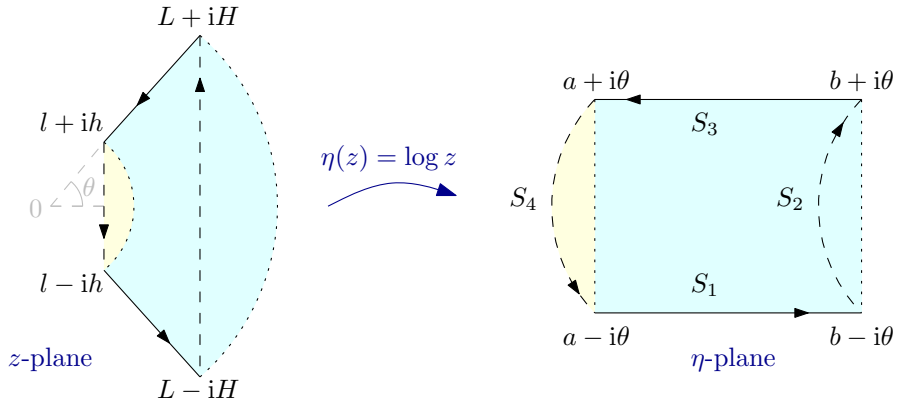

Fig. 5: Extension of domain 2 in the z-plane and its corresponding in the parametric η-plane using the analyticity properties of the Goursat functions.

Using the analyticity of $F_2(\eta)$ and $G_2(\eta)$, it follows that

$$\begin{aligned}\int_{b-\mathrm{i}\theta}^{b+\mathrm{i}\theta} F_2(\eta)\mathrm{e}^{-\mathrm{i}k\eta}\mathrm{d}\eta &= \int_{S_2} F_2(\eta)\mathrm{e}^{-\mathrm{i}k\eta}\mathrm{d}\eta = \sigma_2(k),\\ \int_{a+\mathrm{i}\theta}^{a-\mathrm{i}\theta} F_2(\eta)\mathrm{e}^{-\mathrm{i}k\eta}\mathrm{d}\eta &= \int_{S_4} F_2(\eta)\mathrm{e}^{-\mathrm{i}k\eta}\mathrm{d}\eta = \sigma_4(k)\end{aligned} \tag{6.21}$$

and

$$\begin{aligned}\int_{b-\mathrm{i}\theta}^{b+\mathrm{i}\theta} G_2(\eta)\mathrm{e}^{-\mathrm{i}k\eta}d\eta &= \int_{S_2} G_2(\eta)\mathrm{e}^{-\mathrm{i}k\eta}d\eta = \hat{\sigma}_2(k),\\ \int_{a+\mathrm{i}\theta}^{a-\mathrm{i}\theta} G_2(\eta)\mathrm{e}^{-\mathrm{i}k\eta}d\eta &= \int_{S_4} G_2(\eta)\mathrm{e}^{-\mathrm{i}k\eta}d\eta = \hat{\sigma}_4(k).\end{aligned} \tag{6.22}$$

Using (6.21) and (6.22), it follows that we can write the following integral representations (**16**, **25**) in the rectangular sub-domain $a \le \mathrm{Re}[\eta] \le b$, $-\theta \le \mathrm{Im}[\eta] \le \theta$ in the η-plane:

$$\begin{aligned}F_2(\eta) &= \frac{1}{2\pi}\left[\int_0^{\infty}\sigma_1(k)\mathrm{e}^{\mathrm{i}k\eta}\mathrm{d}k + \int_0^{-\mathrm{i}\infty}\sigma_2(k)\mathrm{e}^{\mathrm{i}k\eta}\mathrm{d}k + \int_0^{-\infty}\sigma_3(k)\mathrm{e}^{\mathrm{i}k\eta}\mathrm{d}k + \int_0^{\mathrm{i}\infty}\sigma_4(k)\mathrm{e}^{\mathrm{i}k\eta}\mathrm{d}k\right],\\ G_2(\eta) &= \frac{1}{2\pi}\left[\int_0^{\infty}\hat{\sigma}_1(k)\mathrm{e}^{\mathrm{i}k\eta}\mathrm{d}k + \int_0^{-\mathrm{i}\infty}\hat{\sigma}_2(k)\mathrm{e}^{\mathrm{i}k\eta}\mathrm{d}k + \int_0^{-\infty}\hat{\sigma}_3(k)\mathrm{e}^{\mathrm{i}k\eta}\mathrm{d}k + \int_0^{\mathrm{i}\infty}\hat{\sigma}_4(k)\mathrm{e}^{\mathrm{i}k\eta}\mathrm{d}k\right].\end{aligned} \tag{6.23}$$

To compute $F_2(\eta)$ and $G_2(\eta)$ in the remaining curvilinear domain bounded by S_4 and $\eta = a + \mathrm{i}\theta s$, $s \in [-1, 1]$ in the η-plane (Figure 5), we construct integral representations for these functions in the corresponding circular domain in the z-plane. Since $F_2(\eta) = f_2(z(\eta))$ and $G_2(\eta) = g_2'(z(\eta))$ can be computed along the vertical side $z = l - \mathrm{i}hs$, $s \in [-1, 1]$ using (6.14), we can write (Crowdy (**28**)):

$$\begin{aligned}f_2(z) =& \frac{1}{2\pi}\int_0^{\mathrm{i}\infty}\upsilon_1(k)\mathrm{e}^{\mathrm{i}kz}\mathrm{d}k\\ &+ \frac{1}{2\pi\mathrm{i}}\left[\int_{L_1}\frac{\upsilon_2(k)}{1-\mathrm{e}^{2\pi\mathrm{i}k}}z^k\mathrm{d}k + \int_{L_2}\upsilon_2(k)z^k\mathrm{d}k + \int_{L_3}\frac{\upsilon_2(k)\mathrm{e}^{2\pi\mathrm{i}k}}{1-\mathrm{e}^{2\pi\mathrm{i}k}}z^k\mathrm{d}k\right],\\ g_2'(z) =& \frac{1}{2\pi}\int_0^{\mathrm{i}\infty}\hat{\upsilon}_1(k)\mathrm{e}^{\mathrm{i}kz}\mathrm{d}k\\ &+ \frac{1}{2\pi\mathrm{i}}\left[\int_{L_1}\frac{\hat{\upsilon}_2(k)}{1-\mathrm{e}^{2\pi\mathrm{i}k}}z^k\mathrm{d}k + \int_{L_2}\hat{\upsilon}_2(k)z^k\mathrm{d}k + \int_{L_3}\frac{\hat{\upsilon}_2(k)\mathrm{e}^{2\pi\mathrm{i}k}}{1-\mathrm{e}^{2\pi\mathrm{i}k}}z^k\mathrm{d}k\right],\end{aligned} \tag{6.24}$$

where

$$\begin{aligned}\upsilon_1(k) &= \int_{l+\mathrm{i}h}^{l-\mathrm{i}h} f_2(z)\mathrm{e}^{-\mathrm{i}kz}\mathrm{d}z, \qquad \upsilon_2(k) = \int_C f_2(z)z^{(-k-1)}\mathrm{d}z,\\ \hat{\upsilon}_1(k) &= \int_{l+\mathrm{i}h}^{l-\mathrm{i}h} g_2'(z)\mathrm{e}^{-\mathrm{i}kz}\mathrm{d}z, \qquad \hat{\upsilon}_2(k) = \int_C g_2'(z)z^{(-k-1)}\mathrm{d}z\end{aligned} \tag{6.25}$$

and where the set $\{L_j|j=1,2,3\}$ constitutes the fundamental contour for circular edges (Crowdy (**28**)). The contour L_1 is the union of the negative imaginary axis $(-\mathrm{i}\infty,-\mathrm{i}r]$, where $0<r<1$, and the arc of the quarter circle $|k|=r$ in the third quadrant traversed in a clockwise sense; the contour L_2 is the real interval $[-r,\infty)$; the contour L_3 is the arc of the quarter circle $|k|=r$ in the second quadrant traversed in a clockwise sense together with the portion of the positive imaginary axis $[\mathrm{i}r,\mathrm{i}\infty)$.

Polygonal domain 3: Finally, the spectral functions $\tau_3(k)$, $\hat{\tau}_3(k)$ can be computed using (6.18). The spectral functions $\tau_j(k)$, $\hat{\tau}_j(k)$, $j=1,2$ follow from back substitution into various relations and the global relations (4.27), (4.30). The correction functions $f_3(z)$, $g_3'(z)$ can be computed using (4.25) and (4.28) respectively. Finally, the Goursat functions $f(z)$ and $g'(z)$ in domain 3 can be computed using (4.22).

7. Results

Once we have computed the Goursat functions $f(z)$ and $g'(z)$ in each domain, physical quantities of interest such as the velocity, pressure and vorticity follow from (2.5). We focus on the effect of the expansion on the pressure drop between the two vertical sides of domain 2.

To compute the pressure in domain 2 which was mapped to the parametric η-plane, we use the chain rule:

$$p = 4\mu\ \mathrm{Re}[f_2'(z)] = 4\mu\ \mathrm{Re}\left[\frac{F_2'(\eta)}{z'(\eta)}\right], \tag{7.1}$$

where dash denotes differentiation with respect to the function variable. Furthermore, to compute the pressure along the vertical edges of domain 2 (which correspond to sides S_2, S_4 in the η-plane), we can use (6.12) and (6.14) to write

$$p\Big|_{z(\eta_j(s))} = 4\mu\ \mathrm{Re}\left[\frac{\mathcal{F}_j'(s)}{z'(\eta_j)\ \eta_j'(s)}\right], \qquad \text{for } \ j=2,4, \quad \text{and} \quad s\in[-1,1], \tag{7.2}$$

where, again, dash denotes differentiation with respect to the function variable.

The pressure drop along the channel centreline between the two ends of the expansion/constriction region is

$$\Delta p = p\Big|_l - p\Big|_L = p\Big|_{z(\eta_4(0))} - p\Big|_{z(\eta_2(0))}. \tag{7.3}$$

The nondimensionalised pressure drop ΔP is defined to be

$$\Delta P = \frac{\Delta p\ H^3}{\mu q_0 L_0}, \tag{7.4}$$

where $L_0 = L - l$ is the length of the expansion/constriction and $q_0 = Q/2$ (the total flow rate in the channel is Q).

We aim to compare our computed values for the dimensionless pressure drop to Tavakol *et al.* (**14**) extended lubrication theory (ELT). Details of the latter are presented in Appendix A, where it is shown that the dimensionless pressure drop is

$$\Delta P = \Delta P_0 + \delta^2 \Delta P_2 + \delta^4 \Delta P_4 + \mathcal{O}(\delta^6), \tag{7.5}$$

where

$$\Delta P_0 = \frac{3}{2}\cdot\frac{1+\nu}{\nu^2}, \quad \Delta P_2 = \frac{21}{10}\cdot\frac{(1+\nu)(1-\nu)^2}{\nu^2}, \quad \Delta P_4 = \frac{159}{350}\cdot\frac{(1+\nu)(1-\nu)^4}{\nu^2}, \tag{7.6}$$

with $\nu = h/H$.

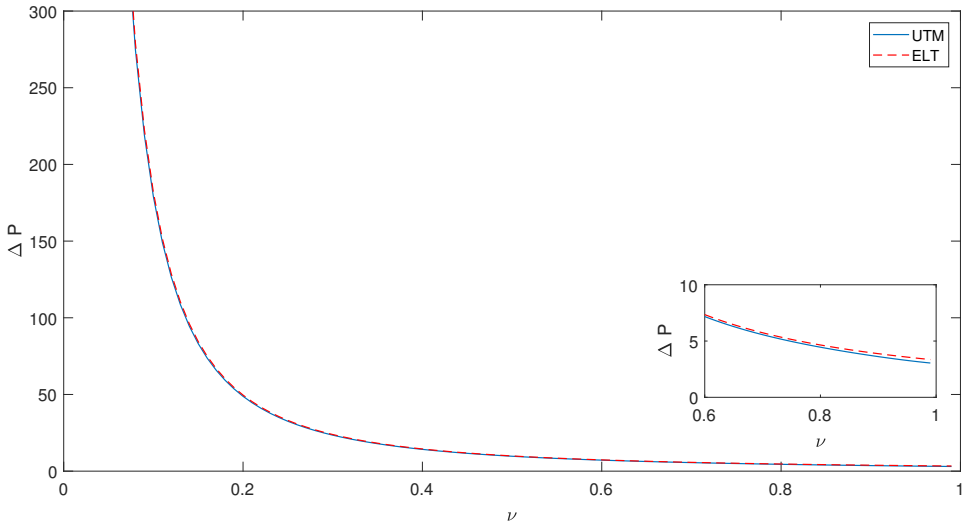

Fig. 6: Comparison of the dimensionless pressure drop between the Unified Transform Method (UTM) and extended lubrication theory (**14**) (ELT) as a function of channel width ratio $\nu = h/H$. The sums (6.12) and (6.14) were truncated to include only terms up to $M = 20$. The results are shown for angle $\theta = \pi/12$. As $\nu \to 0$ (which corresponds to small δ) extended lubrication theory provides an accurate approximation and transform method tends to exact result form. As $\nu \to 1$, the expansion/constriction region tends to disappear and both methods tend to the dimensionless pressure drop $\Delta P = 3/\nu^3 \to 3$ for a channel of constant width $h = H$.

Figure 6 shows the nondimensional pressure drop ΔP between the two ends of the expansion/constriction region along the channel centreline as a function of channel width ratio $\nu = h/H$, $0 < \nu < 1$, for fixed angle $\theta = \pi/12$. The sums (6.12) and (6.14) were truncated to include only terms up to $M = 20$. Our results are compared to Tavakol *et al.* (**14**) extended lubrication theory and the two methods agree. Using the relation

$$\tan\theta = (1-\nu)\delta, \qquad \text{with} \quad \delta = \frac{H}{L-l}, \tag{7.7}$$

we observe that, as $\nu \to 0$ (which corresponds to small δ, since we have assumed that θ is small) extended lubrication theory provides an accurate approximation and transform method converges to that. As $\nu \to 1$, the size of the expansion/constriction region tends

to disappear and both methods tend to the dimensionless pressure drop $\Delta P = 3/\nu^3 \to 3$, corresponding to a channel of constant width $h = H$.

Figure 7 shows the nondimensional pressure drop ΔP between the two ends of the expansion/constriction region along the channel centreline as a function of angle $\theta \in [0, \pi/3]$, for fixed width ratios $\nu = h/H = 0.25, 0.5, 0.75$. The sums (6.12) and (6.14) were again truncated to include only terms up to $M = 20$. Our results are compared to extended lubrication theory. The difference between the two methods becomes significant for angles $\theta > \pi/6$. As stated in (**14**), if the wall slope is too steep, the extended lubrication approach is expected to fail. Although the nondimensional pressure drop values presented in Fig. 7 are for $\theta \in [0, \pi/3]$, our transform approach can also be used to compute the values as $\theta \to \pi/2$. However, in the latter case more terms in the expansions (6.12) and (6.14) are required, as well as an appropriate scaling of the equations to provide good numerical conditioning.

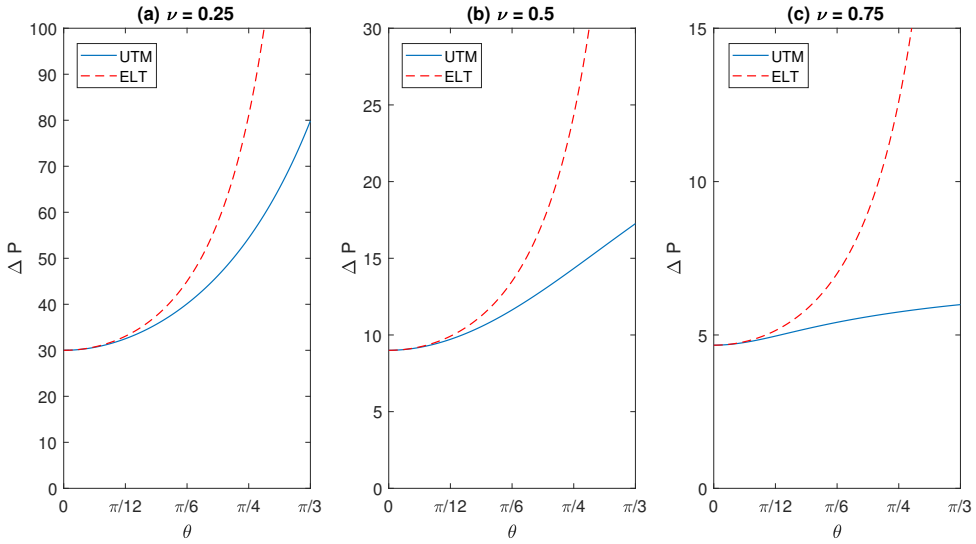

Fig. 7: Comparison of the dimensionless pressure drop between the unified transform method (UTM) and extended lubrication theory (**14**) (ELT) as a function of angle $\theta \in [0, \pi/3]$ for width ratio (a) $\nu = h/H = 0.25$, (b) $\nu = 0.5$ and (c) $\nu = 0.75$. The sums (6.12) and (6.14) were truncated to include only terms up to $M = 20$. The difference between the two methods becomes significant for angles $\theta > \pi/6$.

8. Discussion

We have examined a pressure-driven low-Reynolds-number flow in a two-dimensional channel with a linear expansion and analysed the problem using the Unified Transform Method. Since the transform method can be applied to *convex* polygonal and circular domains, we split the polygonal channel geometry into three convex sub-domains and analysed each of them separately to obtain relations between the so-called spectral functions.

Then, we imposed continuity conditions across common boundaries to couple the sub-problems. The analysis of all the relations between the spectral functions and the use of the global relations offered information on a reduced set of unknown spectral functions at special points in the spectral k-plane; these points encoded the geometry of the problem. Using series expansions to represent unknown boundary data, we formulated and solved a low-order linear system for the unknown coefficients and the two unknown parameters. All the spectral functions followed from back-substitution into the spectral relations.

One of the main advantages of our transform approach over full numerical simulations is that all physical quantities of interest can be computed from the solutions of low-order linear systems. With the coefficients found from these solutions, all the spectral functions appearing in the analytical integral representations for the correction functions $f_j(z)$, $g_j'(z)$, $j = 1, 2, 3$ in each sub-domain can be computed. In addition, the integral expressions for the correction functions are explicit in the variable z (or the mapped variable η), meaning that they can be readily differentiated or integrated to compute quantities of interest. All the aforementioned features emphasise the *quasi-analytical* nature of our solutions.

Our results were compared to extended lubrication theory adapting the analysis of Tavakol *et al.* (**14**) to the channel geometry considered here. We have compared computed values for the pressure drop between the ends of the expansion/constriction region and found that the two methods agree for small angles θ, but differences between them become significant for angles $\theta > \pi/6$. As stated in (**14**), if the wall slope is too steep, the extended lubrication approach is expected to fail.

Acknowledgments

Support from NSF award CMS-1522675 is gratefully acknowledged.

9. References

1. B. J. Kirby, Micro- and Nanoscale Fluid Mechanics: Transport in Microfluidic Devices, Cambridge University Press, New York, (2010).

2. A. M. J. Davis, Periodic blocking in parallel shear or channel flow at low Reynolds number, *Phys. Fluids*, **5**, 800–809, (1993).

3. V. T. Buchwald and H. E. Doran, Eigenfunctions of plane elastostatics II. A mixed boundary value problem of the strip, *Proc. Roy. Soc. Ser. A*, **284**, 69–82, (1965).

4. R. M. L. Foote and V. T. Buchwald, An exact solution for the stress intensity factor for a double cantilever beam, *Int. J. Fracture*, **29**, 125–134, (1985).

5. J-T. Jeong, Slow viscous flow in a partitioned channel, *Phys. Fluids*, **13**, 1577, (2001).

6. I. D. Abrahams, A. M. J. Davis, S. G. Llewellyn Smith, Asymmetric channel divider in Stokes flow, *SIAM J. Appl. Math.*, **68**, 1439–1463, (2008).

7. M-U. Kim & M. K. Chung, Two-dimensional slow viscous flow past a plate midway between an infinite channel, *J. Phys. Soc. Japan*, **53**, 156-166, (1984).

8. T. N. Phillips, Singular matched eigenfunction expansions for Stokes flow around a corner, *IMA J. Appl. Math.*, **42**, 13–26, (1989).

9. A. Setchi, A. J. Mestel, K. H. Parker & J. H. Siggers, Low-Reynolds-number flow through two-dimensional shunts, *J. Fluid Mech.*, **723**, 21–29, (2013).

10. C. Pozrikidis, Boundary Integral and Singularity Methods for Linearized Viscous Flow, New York, NY, Cambridge University Press, (1992).

11. C. Pozrikidis, Creeping flow in two-dimensional channels, *J. Fluid Mech.*, **180**, 495–514, (1987).
12. S. Howison, Practical Applied Mathematics: Modelling, Analysis, Approximation, Cambridge, UK, Cambridge University Press, (2005).
13. H. Ockendon & J. R. Ockendon, Viscous flow, Cambridge, UK, Cambridge University Press, (1995).
14. B. Tavakol, G. Froehlicher, D. P. Holmes & H. A. Stone, Extended lubrication theory: improved estimates of flow in channels with variable geometry, *Proc. R. Soc. A*, **473**, 20170234, (2017).
15. A. S. Fokas, A unified transform method for solving linear and certain nonlinear PDEs, *Proc. Roy. Soc. Lond. A*, **453**, 1411–1443, (1997).
16. A. S. Fokas, A unified approach to boundary value problems, CBMS-NSF Regional Conference Series in Applied Mathematics, vol. 78, SIAM, Philadelphia, (2008).
17. D. G. Crowdy & A. S. Fokas, Explicit integral solutions for the plane elastostatic semi-strip, *Proc. R. Soc. Lond. A*, **460**, 1285–1310, (2004).
18. D. G. Crowdy & A. M. J. Davis, Stokes flow singularities in a two-dimensional channel: a novel transform approach with application to microswimming, *Proc. R. Soc. A*, **469**, 20130198, (2013).
19. D. G. Crowdy & E. Luca, Solving Wiener-Hopf problems without kernel factorization, *Proc. R. Soc. A*, **470**, 20140304, (2014).
20. M. Dimakos & A. S. Fokas, The Poisson and the biharmonic equations in the interior of a convex polygon, *Stud. Appl. Math.*, **134**, 456–498, (2015).
21. D. G. Crowdy & S. J. Brzezicki, Analytical solutions for two-dimensional Stokes flow singularities in a no-slip wedge of arbitrary angle, *Proc. R. Soc. A*, **473**, 20170134, (2017).
22. E. Luca & D. G. Crowdy, A transform method for the biharmonic equation in multiply connected circular domains, *IMA J. Appl. Math.*, (to appear).
23. W. E. Langlois, Slow viscous flows, Macmillan, (1964).
24. H. K. Moffatt, Viscous and resistive eddies near a sharp corner, *J. Fluid Mech.*, **18**, 1–18, (1964).
25. A. S. Fokas & A. A. Kapaev, On a transform method for the Laplace equation in a polygon, *IMA J. Appl. Math.*, **68**, 355–408, (2003).
26. D. A. Spence, A class of biharmonic end-strip problems arising in elasticity and Stokes flow, *IMA J. Appl. Math.*, **30**, 107–139, (1983).
27. W. R. Dean & P. E. Montagnon, On the steady motion of viscous liquid in a corner, *Proc. Camb. Philos. Soc.*, **45**, 389–394, (1949).
28. D. G. Crowdy, Fourier-Mellin transforms for circular domains, *Comput. Methods Funct. Theory*, **15**, 665–687, (2015).

APPENDIX A

Extended lubrication theory

We adapt the extended lubrication theory of Tavakol *et al.* (**14**) to the channel geometry considered here. Consider a two-dimensional pressure-driven flow in a channel with shape $y = \pm h(x) = \pm h_0 H(X)$, where $X = x/L_0$, L_0 is the channel length, h_0 is a characteristic channel height, $H(X)$ is a normalised shape function and $\delta = h_0/L_0 \ll 1$. First, we introduce

the dimensionless variables

$$X = \frac{x}{L_0}, \quad Y = \frac{y}{h_0}, \quad U = \frac{u}{q_0/h_0}, \quad V = \frac{v}{q_0/L_0}, \quad P = \frac{p}{\Delta p} = \frac{p}{\mu q_0 L_0/h_0^3}, \tag{A.1}$$

where q_0 denotes the constant flow rate per unit width. The correspondence of the above parameters to the notation used in this paper $h_0 = H$ (largest channel width), $L_0 = L - l$ (length of the expansion/constriction) and $q_0 = Q/2$ (Q is the total flow rate in the channel). The normalised shape function is given by

$$H(X) = \nu + (1-\nu)X, \quad \text{for } 0 \le X \le 1, \quad \text{where } \nu = h/h_0. \tag{A.2}$$

Nondimensional variables (A.1) are substituted to the Stokes equations (2.1) giving

$$\begin{aligned} \frac{\partial U}{\partial X} + \frac{\partial V}{\partial Y} &= 0, \\ \delta^2 \frac{\partial^2 U}{\partial X^2} + \frac{\partial^2 U}{\partial Y^2} &= \frac{\partial P}{\partial X}, \\ \delta^4 \frac{\partial^2 V}{\partial X^2} + \delta^2 \frac{\partial^2 V}{\partial Y^2} &= \frac{\partial P}{\partial Y}, \end{aligned} \tag{A.3}$$

subject to the following boundary conditions

$$U = V = 0 \quad \text{at } Y = \pm H(X), \tag{A.4}$$

$$\frac{\partial U}{\partial Y} = V = 0 \quad \text{at } Y = 0 \tag{A.5}$$

and

$$\int_0^{H(X)} U(X,Y)\mathrm{d}Y = 1. \tag{A.6}$$

Next, we seek a solution of the form

$$\begin{aligned} U(X,Y;\delta) &= U_0(X,Y) + \delta^2 U_2(X,Y) + \delta^4 U_4(X,Y) + \cdots, \\ V(X,Y;\delta) &= V_0(X,Y) + \delta^2 V_2(X,Y) + \delta^4 V_4(X,Y) + \cdots, \\ P(X,Y;\delta) &= P_0(X,Y) + \delta^2 P_2(X,Y) + \delta^4 P_4(X,Y) + \cdots. \end{aligned} \tag{A.7}$$

in (A.3) and obtain the resulting equations.

We omit all the details and report the key expressions at each order. At $\mathcal{O}(1)$:

$$\begin{aligned} U_0(X,Y) &= \frac{3}{2}\left[-\frac{Y^2}{H(X)^3} + \frac{1}{H(X)}\right], \\ V_0(X,Y) &= \frac{3}{2}(1-\nu)\left[-\frac{Y^3}{H(X)^4} + \frac{Y}{H(X)^2}\right], \\ \Delta P_0 &= \frac{3}{2}\cdot\frac{1+\nu}{\nu^2}. \end{aligned} \tag{A.8}$$

At $\mathcal{O}(\delta^2)$:

$$\begin{aligned} U_2(X,Y) &= (1-\nu)^2\left[\frac{3Y^4}{H(X)^5} - \frac{18}{5}\frac{Y^2}{H(X)^3} + \frac{3}{5}\frac{1}{H(X)}\right], \\ \Delta P_2 &= \frac{21}{10}\cdot\frac{(1+\nu)(1-\nu)^2}{\nu^2}. \end{aligned} \tag{A.9}$$

At $\mathcal{O}(\delta^4)$:

$$\begin{aligned} U_4(X,Y) &= (1-\nu)^4\left[-\frac{9}{2}\frac{Y^6}{H(X)^7}+\frac{57}{10}\frac{Y^4}{H(X)^5}-\frac{369}{350}\frac{Y^2}{H(X)^3}-\frac{51}{350}\frac{1}{H(X)}\right], \\ \Delta P_4 &= \frac{159}{350}\cdot\frac{(1+\nu)(1-\nu)^4}{\nu^2}. \end{aligned} \tag{A.10}$$